Facile Access to Various Cores of Thermoresponsive Filomicelles in Water

Nghia P. Truong,[a] John F. Quinn,[a] Athina Anastasaki,[a,b] David M. Haddleton,[a,b] Michael R. Whittaker*[a] and Thomas P. Davis*[a,b]

[a]ARC Centre of Excellence in Convergent Bio-Nano Science & Technology, Monash Institute of Pharmaceutical Sciences, Monash University, Parkville, Melbourne, Victoria 3052, Australia.

[b] Department of Chemistry, University of Warwick, Coventry CV4 7AL, United Kingdom.

Supporting information

ABSTRACT: The preparation of stable filomicelles or nanoparticles with similar morphology to certain worm-shaped bacteria, viruses, and fungi found in nature has opened the doors to many applications including, but not limited to, tissue engineering and nanomedicines. However, the facile synthesis of filomicelles with high stability in water and variable core properties still remains a major challenge. Herein we report a novel library of highly stable worm-like nanoparticles comprising either styrene or various methacrylate cores. This library is prepared directly in aqueous solution via reversible addition fragmentation chain transfer (RAFT)-mediated emulsion polymerization and temperature-induced morphological transformation (TIMT). The filomicelle products demonstrate reproducibly uniform morphology while exhibiting a broad range of glass transition temperatures, high stability in buffer, and the ability to form smart reversible thermoresponsive gels. The broad-ranging properties of these filomicelles promise a diverse range of industrial and biomedical applications.

Advances in the preparation of stable filomicelles or worm-like nanoparticles (WLN) in water have opened the doors to a variety of novel applications ranging from templated fabrication of nanodevices, formation of three-dimensional superstructures, viscosity modification, nanoreactor assembly, through to tissue engineering and nanomedicine.[1] Significantly, recent studies into nanoscale drug delivery using filomicelles as nanocarriers have demonstrated that synthetic worm-like nanoparticles (WLN) exhibit similar pharmacokinetics compared to certain worm-shaped bacteria, viruses, and fungi found in nature.[2] On a different note, synthetic WLN can form reversible gels via topological interactions, which represents a useful alternative to traditional permanently-crosslinked gels.[3] The unique features of worm-like morphology have been stimulating efforts to develop facile and versatile approaches for producing stable filomicelles in water with greater control over length, surface chemistry, and core properties, thereby enabling their use in a wider array of applications.[4]

The physical properties (e.g., flexibility) of filomicelle cores play an important role in their fragmentation, pharmacokinetics, interactions with biological systems, and as a result, their likely utility.[5] As such, producing stable WLN in water with a variety of core properties would be very useful for a number of potential applications.[6] To date, only a limited number of monomers have been employed to prepare the hydrophobic core of worm-like micelles via RAFT-mediated polymerization in aqueous solution.[7] In particular, only styrene (STY) has been successfully applied for the production of WLN in water by both the polymerization-induced self-assembly (PISA) and temperature-induced morphological transformation (TIMT) techniques.[8] Aside from styrene, 2-hydroxypropyl methacrylate (HPMA) was the first and the only methacrylate monomer utilized for the efficient synthesis of filamentous micelles in aqueous solution via the PISA mechanism.[9] This pioneering work by Armes and coworkers has created a novel paradigm for the production of worm-like micelles directly in water, which is particularly promising for a number of biomedical applications. That said, the synthesis of filomicelles with various methacrylic cores in water by the aqueous RAFT-mediated polymerization remains a long-standing challenge, hampering the broad deployment of this synthesis technique.[10]

In this study, we aim to overcome this synthesis challenge by using the RAFT-mediated emulsion polymerization of a set of methacrylate monomers followed by the TIMT approach to provide, for the first time, an extensive library of filamentous micelles in water with various cores. Initially, the kinetics of RAFT-mediated emulsion polymerization of benzyl methacrylate in aqueous solution were studied to examine whether poly((di(ethylene glycol) methyl ether methacrylate)$_{30}$-co-*N*-(2-hydroxypropyl) methacrylamide)$_7$) (P(DEGMA$_{30}$-co-HPMA$_7$)-SC(=S)SC$_2$H$_5$) was a suitable macro-CTA for controlling the polymerization of methacrylate monomers (see Scheme S1 and Figures S1-S2). The cloud point temperature (T_{cp}) of this macro-CTA was 41 °C and was chosen such that the P(DEGMA$_{30}$-co-HPMA$_7$) would provide a water-soluble corona stabilizing methacrylate WLN at 37 °C (i.e., human body temperature). The conversion of the emulsion polymerization rapidly reached 94% after polymerizing at 60 °C for 3.5 h (see Figure S3A), which reflects a very high rate of polymerization due to the compartmentalization of hydrophobic methacrylate monomer inside the core of the formed nanoaggregates.[11] Importantly, SEC analysis revealed a linear increase in number-average molecular weight (M_n) with increasing conversion, indicating the success of the chain extension reaction (see Figure S3B). Further, the low dispersities ($Đ \leq 1.2$, see Figure S3B) and symmetric molecular weight distributions (MWDs, see Figure S3C) of the formed diblock copolymers suggest a "well-controlled" polymerization proceeding under the RAFT mechanism. Altogether, this kinetic study confirms the successful synthesis of a well-defined PBzMA diblock copolymer by RAFT-mediated emulsion polymerization.

After the polymerization of BzMA, the hot white suspension or latex of the well-defined PBzMA diblock copolymer was then used for the systematic TIMT study to determine whether worm-like morphology of PBzMA nanoaggregates could be obtained by this technique. Specifically, hot latex at 60 °C was cooled to room temperature (23 °C) in the presence and absence of added benzyl methacrylate monomer (20 µL, 40 µL, and 80 µL per 1 mL of latex). The transmission electron microscopy (TEM) image in Figure 1A shows large spherical aggregates when cooling from 60 °C to room temperature (i.e., from above to below the T_{cp} of P(DEGMA$_{30}$-co-HPMA$_7$)) without adding BzMA. This morphology was identical to that of PBzMA diblock copolymer at 60 °C (see Figure S4). These results demonstrated that with only the small amount of unreacted BzMA monomer (i.e., ~ 2 µL per 1 mL of latex), no morphology transformation occurred. In contrast, when cooling from 60 °C to 23 °C in the presence of various amounts of added benzyl methacrylate, the morphology of the PBzMA aggregates transformed from large sphere (~1.3 µm) to (i) small sphere (~ 35 nm, with 20 µL mL^{-1} of added BzMA, see Figure 1B), (ii) filamentous micelle (with 40 µL mL^{-1} of added BzMA, see Figure 1C), or (iii) large vesicle (with 80 µL mL^{-1} of added BzMA, see Figure 1D). In the presence of added BzMA, the morphological transformations observed in Figure 1 were induced by the change in amphiphilicity of the thermoresponsive block from hydrophobic to hydrophilic (or from water-insoluble to water-soluble) when cooling from above to below the T_{cp} of the macro-CTA (see Scheme 1).[7b] However, when BzMA was not added, the change in amphiphilicity was not sufficient to restructure the kinetically-frozen PBzMA core at room temperature (the T_g of the PBzMA core is 51 °C). It is interesting to note that the added BzMA not only functions as a plasticizer for the PBzMA core (i.e., an additive that can increase the chain flexibility of the PBzMA core), but also serves to increase the volume of the hydrophobic chain (v, see equation 1), enabling the formation of the various morphologies of PBzMA nanoaggregates observed in Figure 2.[12] The trend in the observed morphological transformation can be explained using the packing parameter (p) theory described by equation 1:[13]

$$p = v/al \quad (1)$$

where p is the packing parameter; v is the volume of hydrophobic chains; a is the effective interfacial area at the hydrophobic–water interface; and l is the length of the hydrophobic chains.

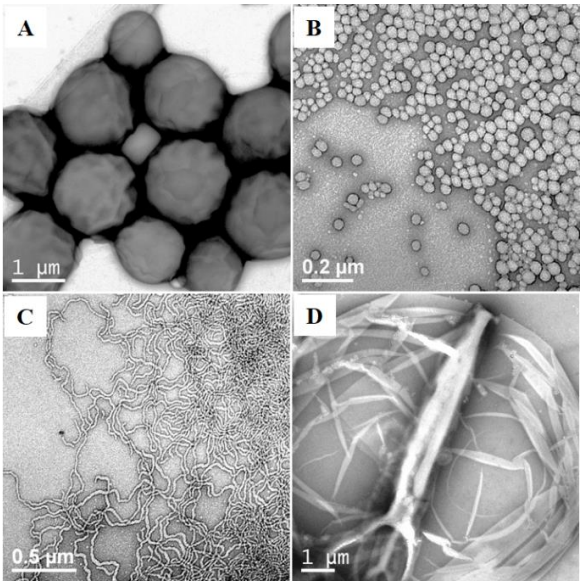

Figure 1. Representative TEM images of the latexes of PBzMA diblock copolymer in water after: 3.5 h of polymerization at 60 °C, subsequent addition of different amounts of benzyl methacrylate (A) 0 µL/mL, (B) 20 µL/mL, (C) 40 µL/mL, (D) 80 µL/mL, and cooling to room temperature (23 °C) overnight. All samples were negatively stained with uranyl formate solution (2 wt% in MilliQ water).

Scheme 1. 3D cartoon representing the formation of PBzMA nanoaggregates with different morphologies in water via temperature-induced morphological transformation (TIMT).

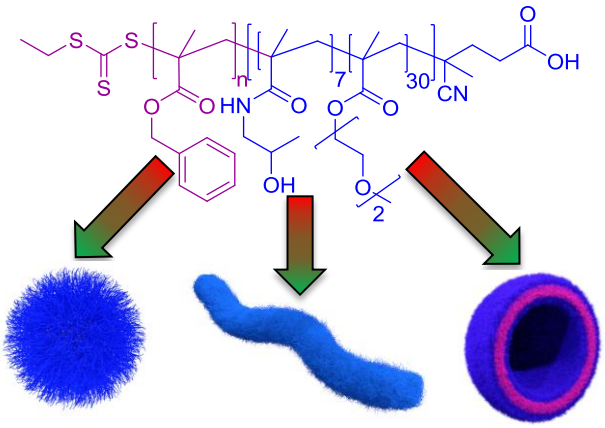

From the packing parameter theory, the increased v caused by the addition of BzMA results in an increased value of p and the corresponding morphological transformation from sphere to cylinder and then to vesicle.[6b,14] It is important to note that the conversion of the polymerization affects both the length of the hydrophobic chain (l) and the volume of hydrophobic chains (v), and as such the formed morphologies. Therefore, similar and high conversions (i.e., >90%) should be reached to reproducibly obtain uniform morphologies. In summary, PBzMA nanoaggregates with various shapes (including filomicelle) have been successfully prepared for the first time in aqueous solution at relatively high solid content (i.e., ~7.5 wt %) via the RAFT-mediated polymerization followed by the application of TIMT.

To expand the scope of this technique, a series of methacrylate monomers that have never been used for the preparation of filomicelles in water including methyl methacrylate (MMA), ethyl methacrylate (EMA), propyl methacrylate (PMA), and butyl methacrylate (BMA) was chosen for a further study (see scheme S2A). These monomers represent a wide range of hydrophobicity (due to the increasing length of hydrocarbon side chain) and, if successful, would form novel WLN with different core physical properties (i.e., T_g). Importantly, the RAFT-mediated emulsion polymerization of BzMA followed by TIMT was repeated (without taking samples for kinetics) to study the reproducibility of both polymer synthesis and filomicelle preparation. Styrene was also investigated as a hydrophobic monomer in this study to target the first library of worm-like micelles with both methacrylic and styrenic cores and to compare the final worm-like morphology obtained with that of filomicelles with methacrylic cores (see Scheme S2B). Altogether, six hydrophobic monomers were used for the emulsion polymerizations in this study (see Table S1). Importantly, the same volume of monomers and the same amount of macro-CTA were used for the polymerizations of each methacrylate (see details of experimental in SI). The difference in the feed ratio of monomer to macro-CTA, and the final degree of polymerization (DP), is the result of the variation in density and molecular mass of the monomer investigated. The increase in M_n after all polymerizations (compared to the M_n of the macro-CTA, see Table S1 and Figures S5-S10) and the presence of signals corresponding to the protons of the hydrophobic components in the ^{1}H NMR spectra of purified products (see Figures S11-S16) indicate that all chain extension polymerizations were successful. In addition, the M_n and $Đ$ of the PBzMA diblock copolymer (P4) is similar to that obtained in the previous polymerization performed for kinetic study (17,600 g/mol and 1.19, respectively). This result attests to the reproducibility of the RAFT-mediated polymerizations reported here.

After polymerization, each hot latexes was cooled to room temperature (23 °C) in the presence of a suitable plasticizer (40

μL mL^{-1}) to study the formation of WLN via TIMT (see Scheme 2). We found that the suitable plasticizer for each polymethacrylate latexes was the monomer used for its polymerization, while toluene was used as the plasticizer for the PSTY latex.[7b] Importantly, TEM images (see Figure 2A-E) show the formation of filomicelle morphology for not only PSTY and PBzMA but also for PMMA, PEMA, and PPMA cores. It is worth noting that filomicelles with MMA, EMA, and PMA cores have never been synthesized by any other method. These results attest to the reproducibility and the versatility of the TIMT approach. However, in the case of PBMA, only spherical morphology was observed (see Figure S16). All further attempts to change the volume of added plasticizer (i.e., the amount of added BMA), the feed ratios (to target different M_n of PBMA diblock copolymers), and the transformation temperature (cooled to, and incubated at 4 °C) still resulted in a spherical shape for PBMA nanoaggregates (similar to the spherical morphology in Figure S16, data not shown). We attribute the spherical morphology observed for PBMA nanoparticles to the low rigidity (i.e., low T_g, see Table 1) of the PBMA core, though further studies are needed to fully understand the relationship between core properties (i.e., rigidity) and the final morphology. The packing parameter theory alone does not give an adequate account of this relationship. That said, those polymers with T_gs from 31 °C to 101 °C (see Table 1) can form stable cores of WLN independently of the specific chemistry of the cores (i.e., styrene or methacrylate). This broad range of T_g choices provides a useful handle for producing filomicelles with various core properties. Given the variety of methacrylate monomers that have T_g higher than 31 °C, using the RAFT-mediated polymerization and TIMT approach reported here would dramatically expand the current library of possible filomicelle cores. Moreover, we found that when heating the purified WLN (e.g., PPMA WLN purified by dialysis to remove PMA and SDS, see SI for more details) to 50 °C (a temperature above the T_{cp} of the P(DEGMA$_{30}$-co-HPMA$_7$)), a stable free-standing gel was formed (e.g., see Figure 2F). This reversible gelling is attributed to the topological interactions of filomicelles.[3c] The worm-like morphology of the nanoaggregates retains after the heating and cooling cycle (e.g., see Figure S18) suggesting the potential utility of these reversible, thermoresponsive gels for tissue engineering applications.[15] In addition, because of the glassy cores and anti-fouling components of the corona (i.e., HPMA and DEGMA), these filomicelles are also stable in phosphate buffered saline for at least a week (see Figure S19), thereby demonstrating considerable potential for use in nanomedicines as nanocarriers.[16]

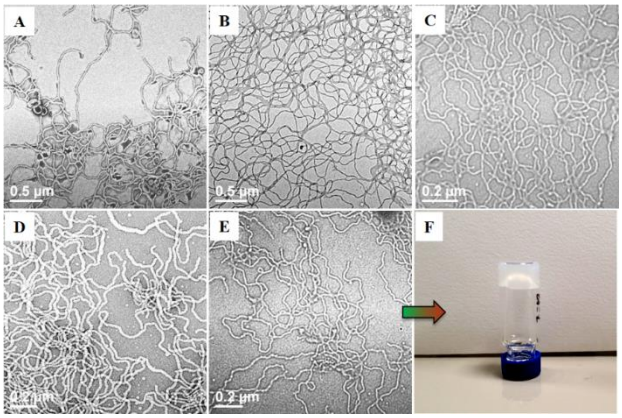

Figure 2. Representative TEM images of the dried latexes of (A) P1, (B) P2, (C) P3, (D) P4, and (E) P5 in water after: emulsion polymerization, subsequent addition of 40 μL/mL of (A) methyl methacrylate, (B) toluene, (C) ethyl methacrylate, (D), benzyl methacrylate and (E) propyl methacrylate, then cooling to room temperature (23 °C) overnight, and finally dialyzing against MilliQ water for 72 h. Samples for (A) P1, (C) P3, (D) P4, and (E) P5 were negatively stained with uranyl formate solution (2 wt% in MilliQ water). (F) Digital photograph recorded for the latex of (E) P4 after dialysis and heating to 50 °C for 1 min.

Scheme 2. A 3D cartoon representing the formation of worm-like nanoparticles in water with different cores via temperature-induced morphological transformation (TIMT).

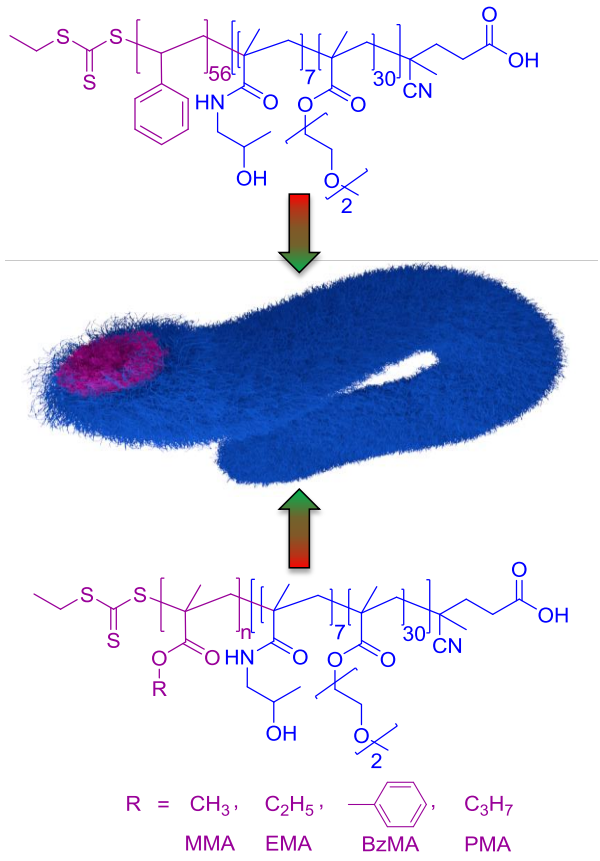

Table 1. Summary of thermoresponsive diblock copolymers synthesized via RAFT-mediated emulsion polymerization in water using AIBN as initiator and P(DEGMA$_7$-co-HPMA$_{30}$)-SC(=S)SC$_2$H$_5$ as macro-CTA.

Copolymer	Monomer	^{1}H NMR		DSC
		DP[a] (n)	M_n[b] (g/mol)	T_g[c] (°C)
P1	MMA	99	17,321	101
P2	STY	56	10,128	95
P3	EMA	85	14,565	61
P4	BzMA	61	10,897	51
P5	PMA	75	12,777	31
P6	BMA	68	11,664	14

[a] Degree of polymerization of styrene was calculated by comparing the ^{1}H NMR intensity of 90 protons of -O-C*H*$_3$ of the DEGMA component (I_j) to the protons of phenyl rings (I_S) using the following equation: $n_{STY} = I_S / I_j * 90 / 5$. Degree of polymerization of MMA was calculated by comparing the ^{1}H NMR intensity of 90 protons of -O-C*H*$_3$ of the DEGMA component (I_i) to the protons of -C(=O)-O-C*H*$_3$ of methacrylate blocks (I_t) using the following equation: $n = I_t / I_i * 90 / 3$. Degree of polymerization (*DP*) of EMA, BzMA, PMA, and BMA were calculated by comparing the ^{1}H NMR intensity of 90 protons of -O-C*H*$_3$ of the DEGMA component (I_i) to the protons of -C(=O)-O-C*H*$_2$- of methacrylate blocks (I_j) using the following equation: $n = I_j / I_i * 90 / 2$. [b] M_n were calculated using the following equation: $M_n = n \times M_{monomer} + 6087$. [c] Glass transition temperatures (T_g) were determined by identifying the inflection points in final DSC heating curves using Pyris software.

In conclusion, the first extensive library of filomicelles that exhibit a range of core properties has been successfully prepared in water. The filomicelle products are uniform, highly stable in water or buffer, and able to form useful thermoresponsive gels. This work has overcome the long-standing synthesis challenge of producing novel filomicelle nanomaterials by using the RAFT-mediated emulsion polymerization followed by the temperature-induced morphological transformation. The synthesis technique is rapid, reproducible, facile, and suitable for styrene as well as a broad range of methacrylate monomers, opening the doors to the possible synthesis of materially complex and chemically functional WLN. The formed diblock copolymers have unimodal molecular weight distributions, low dispersity even at high conversion, and the ability to form different morphologies. This novel class of worm-like nanomaterials with a broad range of glass transition temperature have potential utility for a variety of industrial and biomedical applications.

ASSOCIATED CONTENT

Supporting Information

The Supporting Information is available free of charge on the ACS publications website
Synthesis and characterization

AUTHOR INFORMATION

Corresponding Author

*E-mail: michael.whittaker@monash.edu.
*E-mail: thomas.p.davis@monash.edu.

ACKNOWLEDGMENT

This work was carried out within the Australian Research Council (ARC) Centre of Excellence in Convergent Bio-Nano Science and Technology (Project No. CE140100036). T.P.D. is grateful for the award of an Australian Laureate Fellowship from the ARC. N.P.T. acknowledges the financial support from the Faculty of Pharmacy and Pharmaceutical Sciences, Monash University.

REFERENCES

(1) (a) Yuan, J. Y.; Xu, Y. Y.; Walther, A.; Bolisetty, S.; Schumacher, M.; Schmalz, H.; Ballauff, M.; Muller, A. H. E. *Nat. Mater.* **2008**, *7*, 718; (b) Wang, H.; Patil, A. J.; Liu, K.; Petrov, S.; Mann, S.; Winnik, M. A.; Manners, I. *Adv. Mater.* **2009**, *21*, 1805; (c) Hudson, Z. M.; Boott, C. E.; Robinson, M. E.; Rupar, P. A.; Winnik, M. A.; Manners, I. *Nat. Chem.* **2014**, *6*, 893; (d) Qiu, H. B.; Hudson, Z. M.; Winnik, M. A.; Manners, I. *Science* **2015**, *347*, 1329; (e) Silva, G. A.; Czeisler, C.; Niece, K. L.; Beniash, E.; Harrington, D. A.; Kessler, J. A.; Stupp, S. I. *Science* **2004**, *303*, 1352.
(2) (a) Vacha, R.; Martinez-Veracoechea, F. J.; Frenkel, D. *Nano Lett.* **2011**, *11*, 5391; (b) Shimoni, O.; Yan, Y.; Wang, Y. J.; Caruso, F. *ACS Nano* **2013**, *7*, 522; (c) Truong, N. P.; Whittaker, M. R.; Mak, C. W.; Davis, T. P. *Expert Opin. Drug Deliv.* **2015**, *12*, 129; (d) Geng, Y.; Dalhaimer, P.; Cai, S.; Tsai, R.; Tewari, M.; Minko, T.; Discher, D. E. *Nat. Nanotechnol.* **2007**, *2*, 249; (e) Barua, S.; Mitragotri, S. *ACS Nano* **2013**, *7*, 9558.
(3) (a) Blanazs, A.; Verber, R.; Mykhaylyk, O. O.; Ryan, A. J.; Heath, J. Z.; Douglas, C. W. I.; Armes, S. P. *J. Am. Chem. Soc.* **2012**, *134*, 9741; (b) Fielding, L. A.; Lane, J. A.; Derry, M. J.; Mykhaylyk, O. O.; Armes, S. P. *J. Am. Chem. Soc.* **2014**, *136*, 5790; (c) Raghavan, S. R.; Douglas, J. F. *Soft Matter* **2012**, *8*, 8539.
(4) (a) Gilroy, J. B.; Gadt, T.; Whittell, G. R.; Chabanne, L.; Mitchels, J. M.; Richardson, R. M.; Winnik, M. A.; Manners, I. *Nat. Chem.* **2010**, *2*, 566; (b) Jia, Z. F.; Bobrin, V. A.; Truong, N. P.; Gillard, M.; Monteiro, M. J. *J. Am. Chem. Soc.* **2014**, *136*, 5824; (c) Wang, X.; Guerin, G.; Wang, H.; Wang, Y.; Manners, I.; Winnik, M. A. *Science* **2007**, *317*, 644; (d) Shuvaev, V. V.; Ilies, M. A.; Simone, E.; Zaitsev, S.; Kim, Y.; Cai, S. S.; Mahmud, A.; Dziubla, T.; Muro, S.; Discher, D. E.; Muzykantov, V. R. *ACS Nano* **2011**, *5*, 6991; (e) Ladmiral, V.; Semsarilar, M.; Canton, I.; Armes, S. P. *J. Am. Chem. Soc.* **2013**, *135*, 13574; (f) Truong, N. P.; Quinn, J. F.; Dussert, M. V.; Sousa, N. B. T.; Whittaker, M. R.; Davis, T. P. *ACS Macro Letters* **2015**, *4*, 381; (g) Jia, Z. F.; Truong, N. P.; Monteiro, M. J. *Polym Chem-Uk* **2013**, *4*, 233.
(5) (a) Mandal, S.; Eksteen-Akeroyd, Z. H.; Jacobs, M. J.; Hammink, R.; Koepf, M.; Lambeck, A. J. A.; van Hest, J. C. M.; Wilson, C. J.; Blank, K.; Figdor, C. G.; Rowan, A. E. *Chem Sci* **2013**, *4*, 4168; (b) Mullner, M.; Dodds, S. J.; Nguyen, T. H.; Senyschyn, D.; Porter, C. J. H.; Boyd, B. J.; Caruso, F. *ACS Nano* **2015**, *9*, 1294; (c) Anselmo, A. C.; Zhang, M.; Kumar, S.; Vogus, D. R.; Menegatti, S.; Helgeson, M. E.; Mitragotri, S. *ACS Nano* **2015**, *9*, 3169.
(6) (a) Charleux, B.; Delaittre, G.; Rieger, J.; D'Agosto, F. *Macromolecules* **2012**, *45*, 6753; (b) Rieger, J. *Macromol. Rapid Commun.* **2015**, *36*, 1458.
(7) (a) Sugihara, S.; Blanazs, A.; Armes, S. P.; Ryan, A. J.; Lewis, A. L. *J. Am. Chem. Soc.* **2011**, *133*, 15707; (b) Truong, N. P.; Whittaker, M. R.; Anastasaki, A.; Haddleton, D. M.; Quinn, J. F.; Davis, T. P. *Polym Chem-Uk* **2016**, DOI: 10.1039/c5py01467k.
(8) (a) Warren, N. J.; Mykhaylyk, O. O.; Mahmood, D.; Ryan, A. J.; Armes, S. P. *J. Am. Chem. Soc.* **2014**, *136*, 1023; (b) Boisse, S.; Rieger, J.; Belal, K.; Di-Cicco, A.; Beaunier, P.; Li, M. H.; Charleux, B. *Chem. Commun.* **2010**, *46*, 1950; (c) Truong, N. P.; Dussert, M. V.; Whittaker, M. R.; Quinn, J. F.; Davis, T. P. *Polym Chem-Uk* **2015**, *6*, 3865; (d) Bauri, K.; Narayanan, A.; Haldar, U.; De, P. *Polym Chem-Uk* **2015**, *6*, 6152.
(9) Blanazs, A.; Madsen, J.; Battaglia, G.; Ryan, A. J.; Armes, S. P. *J. Am. Chem. Soc.* **2011**, *133*, 16581.
(10) (a) Semsarilar, M.; Jones, E. R.; Blanazs, A.; Armes, S. P. *Adv. Mater.* **2012**, *24*, 3378; (b) Warren, N. J.; Armes, S. P. *J. Am. Chem. Soc.* **2014**, *136*, 10174; (c) Ning, Y.; Fielding, L. A.; Andrews, T. S.; Growney, D. J.; Armes, S. P. *Nanoscale* **2015**, *7*, 6691; (d) Cunningham, V. J.; Alswieleh, A. M.; Thompson, K. L.; Williams, M.; Leggett, G. J.; Armes, S. P.; Musa, O. M. *Macromolecules* **2014**, *47*, 5613; (e) Jones, E. R.; Semsarilar, M.; Blanazs, A.; Armes, S. P. *Macromolecules* **2012**, *45*, 5091; (f) Fielding, L. A.; Derry, M. J.; Ladmiral, V.; Rosselgong, J.; Rodrigues, A. M.; Ratcliffe, L. P. D.; Sugihara, S.; Armes, S. P. *Chem Sci* **2013**, *4*, 2081; (g) Semsarilar, M.; Ladmiral, V.; Blanazs, A.; Armes, S. P. *Polym Chem-Uk* **2014**, *5*, 3466; (h) Yeow, J.; Xu, J. T.; Boyer, C. *Acs Macro Letters* **2015**, *4*, 984; (i) Garrett, E. T.; Pei, Y.; Lowe, A. B. *Polym Chem-Uk* **2015**, DOI: 10.1039/C5PY01672J.
(11) Zetterlund, P. B.; Thickett, S. C.; Perrier, S.; Bourgeat-Lami, E.; Lansalot, M. *Chem. Rev.* **2015**, *115*, 9745.
(12) Mangalara, J. H.; Simmons, D. S. *ACS Macro Letters* **2015**, *4*, 1134.
(13) (a) Figg, C. A.; Simula, A.; Gebre, K. A.; Tucker, B. S.; Haddleton, D. M.; Sumerlin, B. S. *Chem Sci* **2015**, *6*, 1230; (b) Patterson, J. P.; Robin, M. P.; Chassenieux, C.; Colombani, O.; O'Reilly, R. K. *Chem. Soc. Rev.* **2014**, *43*, 2412; (c) Derry, M. J.; Fielding, L. A.; Armes, S. P. *Prog. Polym. Sci.* **2015**, DOI:10.1016/j.progpolymsci.2015.10.002.
(14) Holder, S. J.; Sommerdijk, N. A. J. M. *Polym Chem-Uk* **2011**, *2*, 1018.
(15) (a) Buwalda, S. J.; Boere, K. W. M.; Dijkstra, P. J.; Feijen, J.; Vermonden, T.; Hennink, W. E. *J. Controlled Release* **2014**, *190*, 254; (b) Truong, V. X.; Ablett, M. P.; Richardson, S. M.; Hoyland, J. A.; Dove, A. P. *J. Am. Chem. Soc.* **2015**, *137*, 1618.
(16) (a) Christian, D. A.; Cai, S.; Garbuzenko, O. B.; Harada, T.; Allison, L.; Minko, T.; Discher, D. E. *Mol. Pharm.* **2009**, *6*, 1343; (b) Chen, T.; Guo, X.; Liu, X.; Shi, S.; Wang, J.; Shi, C. L.; Qian, Z. Y.; Zhou, S. B. *Adv Healthc Mater* **2012**, *1*, 214.

TOC Graphic

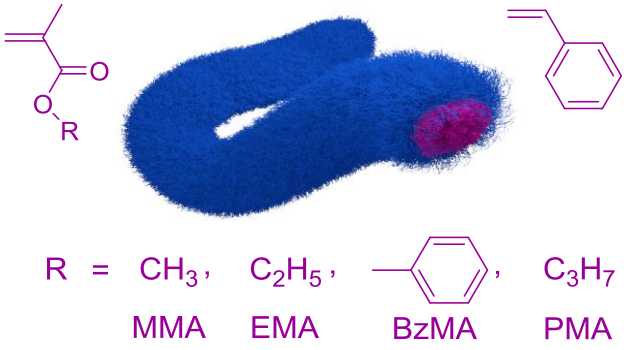

R = CH_3, C_2H_5, , C_3H_7

MMA EMA BzMA PMA